



13th World Conference on Earthquake Engineering
Vancouver, B.C., Canada
August 1-6, 2004
Paper No. 2858

3D TEMPORAL CHARACTERISTICS ANALYSES FOR CHI-CHI EARTHQUAKE GROUND MOTIONS

Junwu DAI¹, Xiaozhai QI², Mai TONG³ and George C. LEE⁴

SUMMARY

Studies of 3D temporal characteristics of earthquake ground motions are definitely motivated by seismic damage to structures. It is well known that six degree-of-freedom-correlated dynamic forces can cause complicated structural damage and the uni-directional based indexes may only capture the damage potential of a ground motion that can be observed in the projected direction. However, most of the currently used ground motion indices largely simply the essential kinematics relationship of the 3D time histories, no longer contain sufficient information to differentiate the various causes and formations of the damage characteristics of the underlying ground motions. In this paper, using the recently developed 3D temporal characteristics analysis, we examine the typical features of 47 near field motion records from Chi-Chi earthquake. Some interesting phenomena are found to be very useful, such as the acceleration pulses are kinematically independent of the velocity PVs and are not the causes of the velocity pulses, the PA of the largest acceleration spike immediately follows the PV of the largest velocity pulse and the large velocity pulse is due to prolonged positive tangential acceleration accumulation. In comparison to the acceleration temporal characteristics, velocity time histories often show more of the ground motion characters that affect a larger area such as wave propagation and attenuation.

INTRODUCTION

As one of the major advances in recent earthquake engineering research, near-field ground motions containing large displacement, velocity and acceleration pulses are recognized as the principal cause of significant damage to structures. While the damaging characteristics of ground motions are apparent in

¹ Professor, Institute of Engineering Mechanics, China Seismological Bureau, P.R. China. Email=iemjwdai@163.com

² Professor, Institute of Engineering Mechanics, China Seismological Bureau, P.R. China. Email=qxz@iem.net.cn

³ Senior Scientist, Multidisciplinary Center for Earthquake Engineering Research, State University of New York at Buffalo, USA.

⁴ Professor, Multidisciplinary Center for Earthquake Engineering Research, State University of New York at Buffalo, USA.

moderate to large earthquakes, the complexity and variation of the focal mechanism coupled with fault rupture and strong site interactions make understanding different types of pulses a difficult task.

The 3D temporal characteristics analysis, including the normal and tangential accelerations and temporal curvature and torsion, is a useful tool to help us look into the unique characteristics of earthquake ground motions even the structural responses. In particular, after taking away the kinematics relations among the acceleration, velocity and displacement time histories, we may find these temporal characteristics particularly helpful for identifying certain nonlinear dynamics involved in the ground motions.

In Tong and Lee (1999), Lee, Tong and Tao (2000) and Tong, Qi and Lee (2001), some basic theoretical background and applications of the 3D temporal characteristics analysis such as for a set of 10 records from Chi-Chi earthquake have been developed. In this paper, we try to evaluate another set of near field Chi-Chi earthquake records from different site conditions by using the 3D temporal characteristics analysis.

GROUND MOTION SELECTION

Chi-Chi earthquake occurred on September 21, 1999, with the epicenter located in central Taiwan. Many reports and investigations related to this earthquake have been carried out in the past 4 years. The general observations and damage evaluations suggest that the causative fault propagated from the south toward the north along an 80 Km fault line. The maximum horizontal displacement was up to 9 m and vertical displacement was up to 1-4 m. Along the fault line, large ruptures and permanent offsets were observed in the north, whereas the severe damages were observed mainly in the south. Many experts believed that the heavy damages were due to the high frequency components in the ground motion in the south. In comparison, the ground motion in the north carried a very low frequency, which produced the fault rupture, but had relatively less impact on buildings and structures. Especially, there are quite number of records with prominent site effects were also observed in this event. As is known, distance to the epicenter is not the only dominant factor for high maximum PGA, we believe that the local area of each station had experienced a unique dynamic process. The ground motion time history records contain specific seismic activities need to be understood.

In the following, we selected 49 Chi-Chi ground motion records with different site conditions to evaluate their 3D temporal characteristics. Table 1 gives out the basic information such as the locations and peak motion information for these records. The selected ground motions can be generally classified as three groups according to the site conditions. The first group consists with 9 records (Chi-1~Chi-9) with the soil condition of shear velocity between 360~750 m/sec. In turn, the second group consists with 33 records (Chi-10~Chi-41) with the soil condition of shear velocity between 180~360 m/sec and the third group consists with 8 records (Chi-41~Chi-49) with the soil condition of shear velocity less than 180 m/sec. Each group has a relatively similar soil condition. Some major aspects to be discussed are:

Amplitude bias for tangential acceleration

Decompositions of large acceleration spikes
 Relations between PGA and PGV
 Duration of acceleration and deceleration

Table 1 Selected ground motion records from Chi-Chi earthquake

Group	Name	Station	Dist(Km)	UD(gal)	NS(gal)	EW(gal)	Latitude	Longitude
I	Chi-1	TCU089	7.5	190.2	225.3	347.8	23.9037	120.8565
	Chi-2	TCU084	10.5	311.8	422.8	989.2	23.883	120.8998
	Chi-3	TCU120	23.2	166.5	193.5	223.0	23.9803	120.6130
	Chi-4	CHY080	31.7	715.9	841.5	792.4	23.5972	120.6777
	Chi-5	CHY074	38.8	97.7	157.0	229.2	23.5103	120.8052
	Chi-6	CHY029	38.9	157.6	233.2	283.0	23.6135	120.5282
	Chi-7	TCU057	39.6	81.5	100.1	111.3	24.1732	120.6107
	Chi-8	TCU045	76.32	353	512	463	24.5417	120.9138
	Chi-9	TCU095	94.43	251	685	367	24.6915	121.0137
II	Chi-10	TCU078	7.1	171	302.5	439.7	23.8120	120.8455
	Chi-11	TCU079	9.9	383.8	417	579.8	23.8397	120.8942
	Chi-12	TCU129	11.9	335	611	983	23.8783	120.6843
	Chi-13	TCU076	13.7	275.4	420	340	23.9077	120.6757
	Chi-14	TCU071	13.9	415.5	639	517.8	23.986	120.7882
	Chi-15	TCU075	18.4	223.9	257.3	325.3	23.9827	120.6778
	Chi-16	TCU074	20.0	270.2	368.4	585.9	23.9622	120.9618
	Chi-17	TCU122	20.0	236	255.6	207.4	23.8128	120.6097
	Chi-18	TCU072	20.6	274.7	370.5	465.3	24.0207	120.8488
	Chi-19	TCU138	21.9	110.4	207.4	202.2	23.9223	120.5955
	Chi-21	CHY024	22.8	141.4	162.2	276.3	23.7570	120.6062
	Chi-22	TCU065	24.6	257.8	563.2	774.4	24.059	120.691
	Chi-23	TCU067	26.8	230.6	312.7	488.9	24.0912	120.7200
	Chi-24	CHY101	30.9	162.2	390	333	23.6862	120.5622
	Chi-25	TCU123	31.4	85.5	132	149	24.0187	120.5437
	Chi-26	CHY028	32.1	336	750	624	23.6327	120.6055
	Chi-27	TCU063	33.2	133	130	179	24.1083	120.6158
	Chi-28	TCU055	33.8	153	208	257	24.1392	120.6643
	Chi-29	TCU109	34.0	133	159	149	24.0848	120.5713
	Chi-30	TCU	34.2	119	187	201	24.1475	120.6760
	Chi-31	TCU082	34.2	129	183	221	24.1475	120.6760
	Chi-32	TCU106	35.3	116	122	157	24.0833	120.5518
	Chi-33	TCU054	35.7	133	190	143	24.1612	120.6750
	Chi-34	TCU051	36.5	110	231	157	24.1603	120.6518
	Chi-35	TCU052	37.9	194	439	349	24.1980	120.7393

	Chi-36	TCU053	39.2	121	132	225	24.1935	120.6688
	Chi-37	TCU050	39.4	87	128	143	24.1815	120.6338
	Chi-38	TCU061	39.7	86	154	133	24.1355	120.5490
	Chi-39	CHY035	43.6	106	244	246	23.5200	120.5840
	Chi-40	TCU102	43.8	173	169	298	24.2493	120.7208
	Chi-41	TCU068	46.3	519	362	502	24.278	120.7657
III	Chi-42	TCU116	22.3	119	133	185	23.8568	120.5803
	Chi-43	TCU110	26.0	116	188	178	23.9622	120.5695
	Chi-44	CHY025	30.5	170	152	159	23.7795	120.5137
	Chi-45	TCU141	34.3	107	89	87	23.8338	120.4640
	Chi-46	TCU115	35.4	76	115	94	23.9595	120.4693
	Chi-47	TCU056	37.6	117	140	154	24.1588	120.6238
	Chi-48	CHY026	40.1	70	66	76	23.7987	120.4113
	Chi-49	CHY104	40.1	130	177	143	23.6695	120.4648

3D TEMPORAL CHARACTERISTICS ANALYSIS

Group One

The soil condition of this group is with the shear velocity between 360~750 m/sec which has the hardest site in selected 3 group motions. From table 1 we can see that the bold marked records have the relatively higher peak values although they are not the closest records to the epicenter in which Chi-2 has the highest peak acceleration, while Chi-1 is the closest record to the epicenter. Chi-9 is most far away (94.43 Km) from the epicenter but it has a quite high peak motion which is much higher than that of Chi-1.

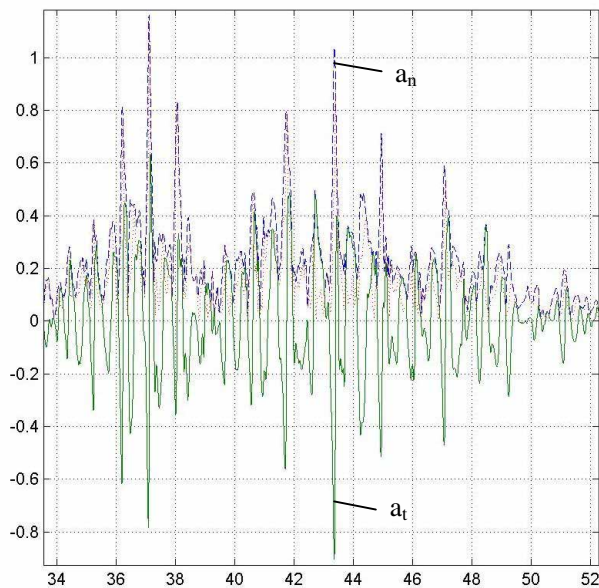


Figure 1 Decomposed a_t and a_n of Chi-2

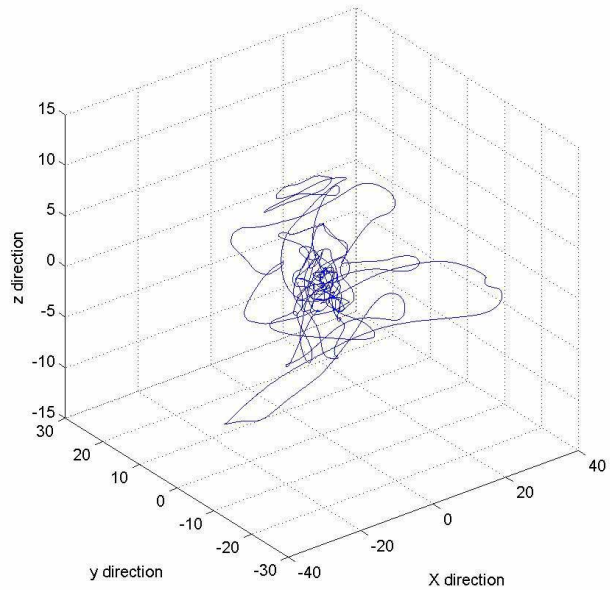


Figure 2 3D displacement trajectory of Chi-2

The decomposition of the Chi-2 acceleration into tangential acceleration a_t and normal acceleration a_n show that large amplitudes of a_t are biased to the negative side (Figure 1). The largest peak deceleration is about 0.93g; whereas the largest peak acceleration is about 0.65g. In addition, the accumulated large deceleration ($<-0.75g$) significantly overwhelmed that of acceleration ($>0.60g$). Figure 3 shows the histogram of large deceleration vs. large acceleration. Examining the maximum PGA and PGV (Figure 2), we can see that maximum PGV occurred at 42.2 seconds, followed by the maximum PGA at 42.3 seconds. The two peak values are kinematically related. The lag of maximum PGA indicates that it is due to a large deceleration, which reduces the maximum PGA occurred a moment earlier. From the displacement trajectory, it is seen that a rapid change of direction had occurred at 42.3 seconds (Figure 3).

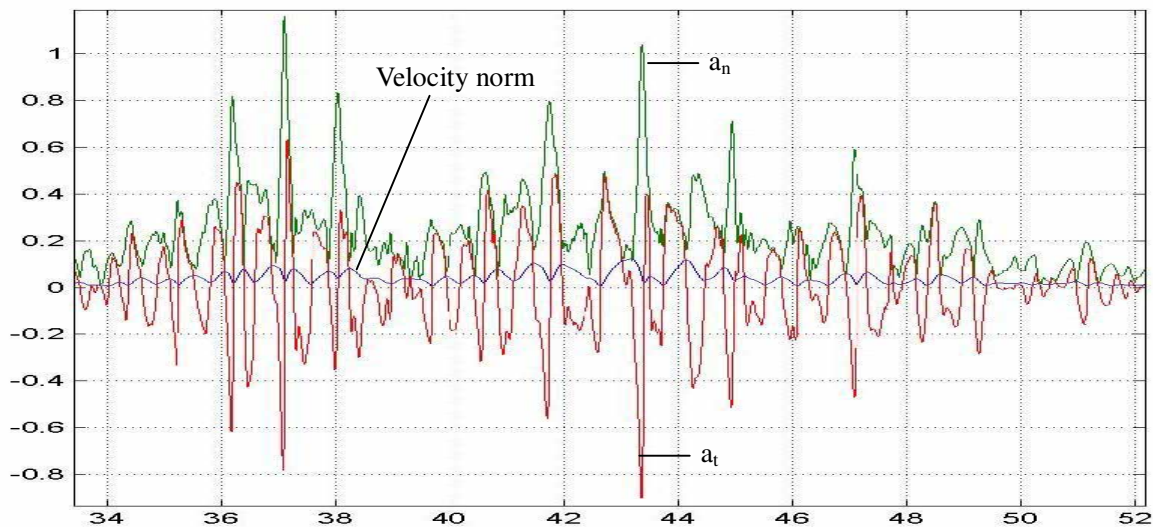


Figure 3 Velocity norm, tangential acceleration a_t and normal acceleration a_n of Chi-2

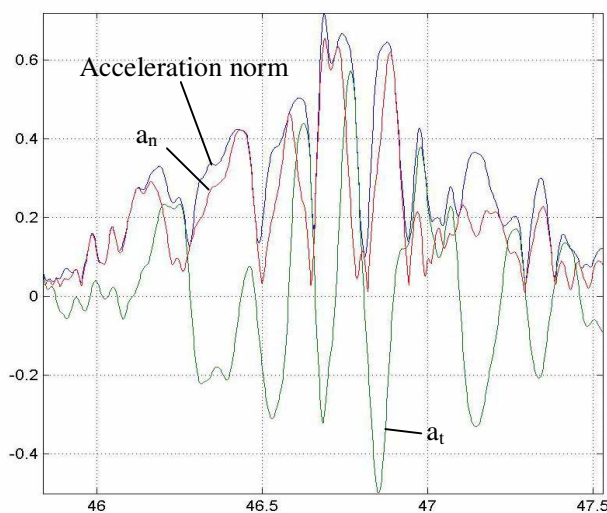


Figure 4 Decomposed a_t and a_n of Chi-9

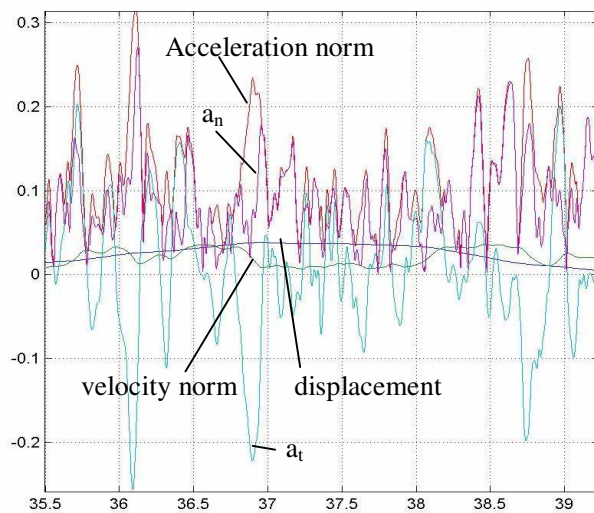


Figure 5 Decomposed a_t and a_n of Chi-1

Figure 4 shows the histogram of large deceleration vs. large acceleration, together with the velocity and displacement norm for record Chi-9 while figure 5 for record Chi-1. Generally, the common feature could be found from these figures is a large acceleration results the increasing of the velocity while the deceleration results the reduction of the velocity norm, and the occurrence time of the peak displacement is strongly related with a lower velocity norm while a lower displacement is not necessary related with a higher velocity norm. Another interesting phenomenon is that the 3D trajectory (figure 6) of these two records (Chi-1 and Chi-9) is quite different. Chi-1 has fewer large displacement pulses than Chi-9 although Chi-1 is much closer to the epicenter.

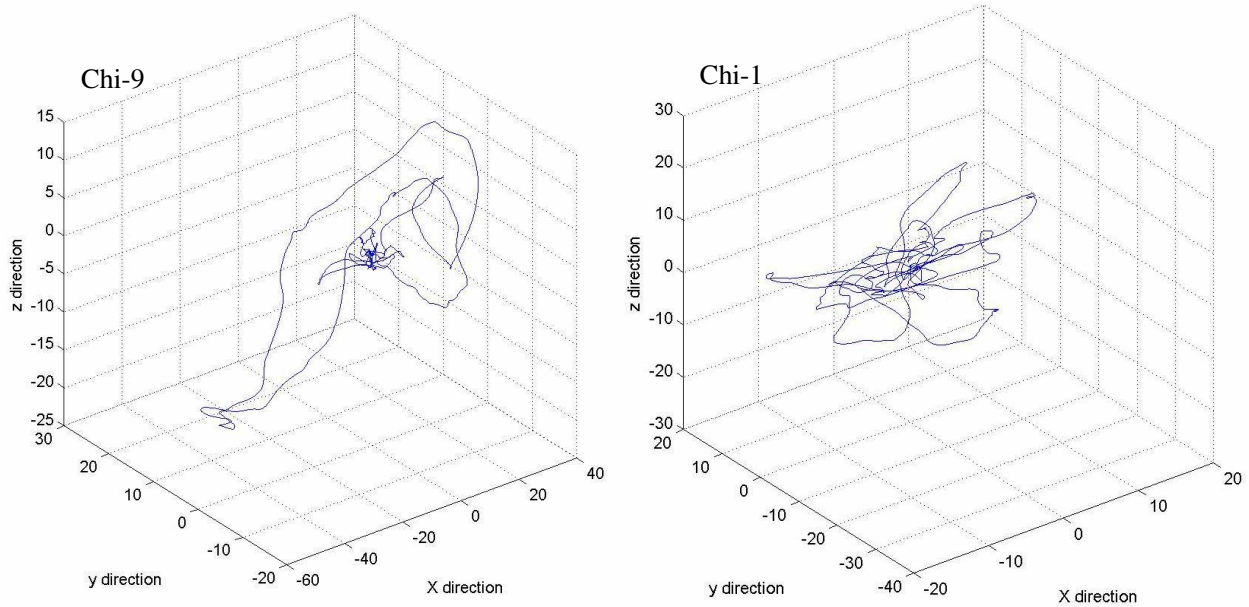


Figure 6 3D displacement trajectory of Chi-9 and Chi-1

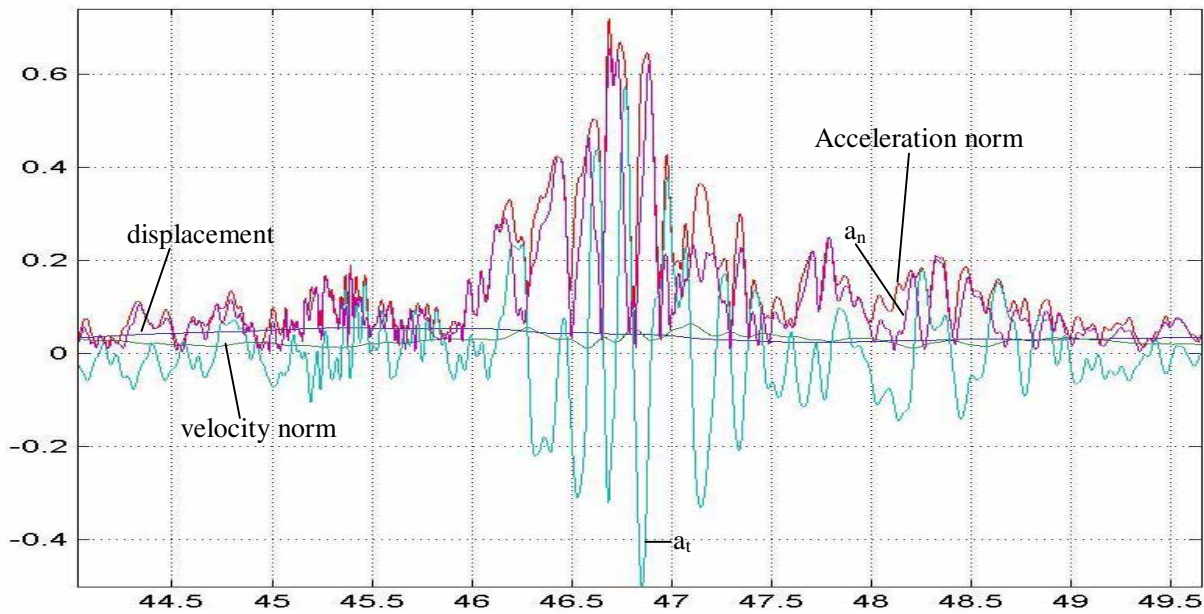


Figure 7 Displacement, velocity norm, tangential a_t and normal a_n of Chi-9

Chi-9: The maximum PGA in this record is 0.71g, but the maximum PGV is only 0.5 m/s. There are several high acceleration and deceleration peaks at approximately the same time when the maximum PGV occurred (Figure 7). The maximum PGA and PGV are kinematically related. The PGA precedes the PGV, which indicates that the accumulation of acceleration in the time interval and that the maximum PGA produced the maximum PGV. The time interval of the acceleration and deceleration is about 0.1 seconds, which is much shorter than that displayed in Chi-41 record in group two.

Group Two

Although the ground motion record in this group (Chi-10~Chi-41) all have much softer soil condition (between 180~360 m/sec) than group one, their temporal characteristics of the time histories have little similarities. Each record possesses some unique properties. Some detailed analysis for Chi-11, Chi-22, Chi-26 and Chi-41 are given out.

Chi-11: The station that recorded Chi-11 is only 9.9 km from the epicenter. It is the second closest to the epicenter among all 32 records in this group. However, the maximum PGA in this group is relatively low but much higher than record Chi-10. It is ranked 8th among the 49 records. The temporal characteristics of Chi-11 are also different from the previous discussed records. The most outstanding aspects are summarized in the following. The a_t and a_n decomposition of the acceleration time history shows that the a_t amplitude distribution is not biased. Maximum PGV, which occurred at 44.5 seconds, is related to the largest acceleration peak (44.3 seconds) and largest deceleration peak (44.6 seconds) (Figure 8). A similar situation in less magnitude occurred at an earlier time (36.6 seconds). In both cases, the acceleration peaks were almost the same as the consequent deceleration peaks.

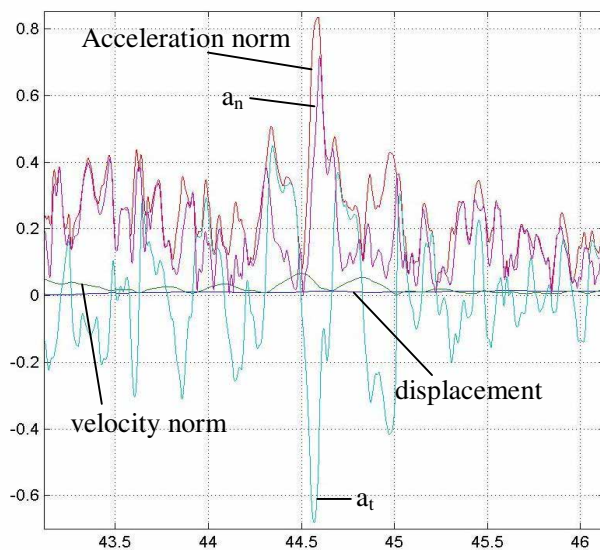


Figure 8 Displacement, velocity norm, tangential a_t and normal a_n of Chi-11

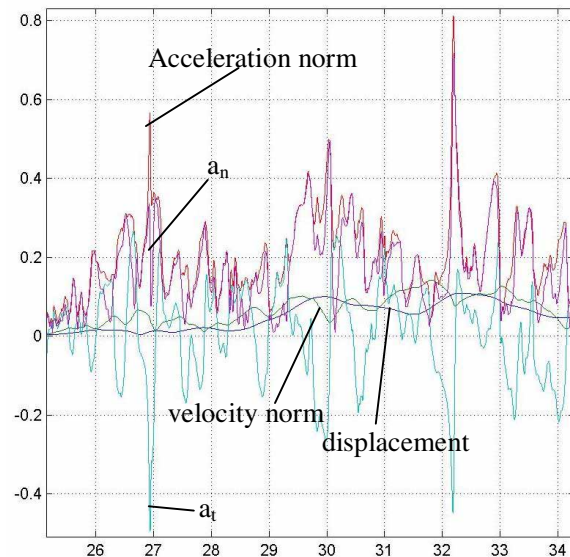


Figure 9 Displacement, velocity norm, tangential a_t and normal a_n of Chi-22

Chi-22: The velocity time histories of record Chi-12, Chi-22 and Chi-41 have something in common. They

all have a high level of velocity during a concentrated period. As shown in Figure 9, the level of high velocity increases as the waves propagate from Chi-12 to Chi-41. However, the tangential acceleration a_t displayed large narrow deceleration peaks. Similar to Chi-2 and Chi-26 and even more severely, the amplitude of a_t is complete biased to the negative (deceleration). The top 50% amplitude of a_t norm ranges from 0.4g to 0.81g, their accumulative duration is 0.15 seconds and are all contributed by deceleration. In particular, compared to Chi-12 (Figure 10) and Chi-41, only Chi-22 has such deceleration peaks despite the similarity among the velocity time histories. These peaks even repeated several times throughout the Chi-22 time history. This suggests that the same dynamic process dominates the responses in this local area. It is interesting to note that such peaks have little influence on the velocity time history. In fact, the maximum PGV and PGA in this record are kinematically unrelated, which suggests that neither the maximum PGA is caused by integration of the maximum PGA, nor the maximum PGA is caused by derivative of the maximum PGV.

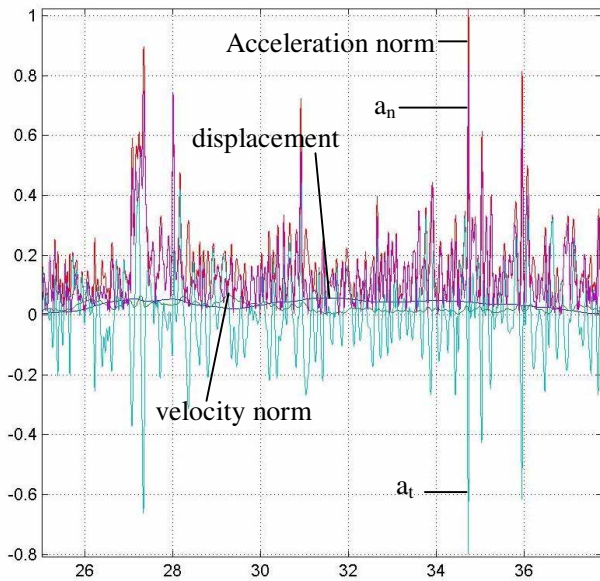


Figure 10 Displacement, velocity norm, tangential a_t and normal a_n of Chi-12

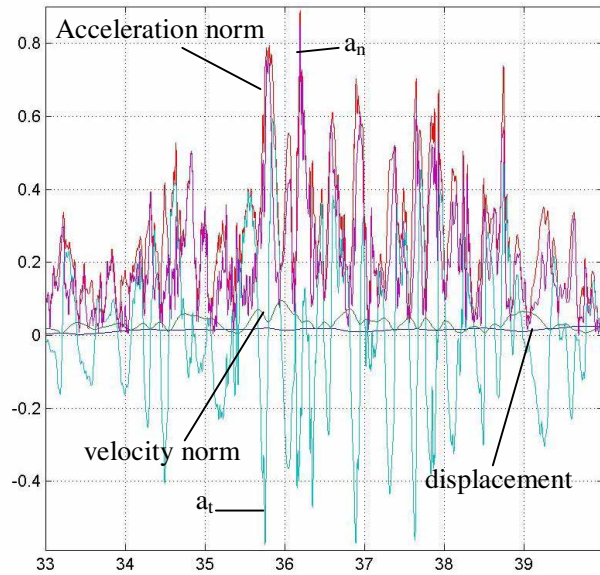


Figure 11 Displacement, velocity norm, tangential a_t and normal a_n of Chi-26

Chi-26: This record has similar characteristics as Chi-2, that is, large deceleration peaks dominate the acceleration norm (Figure 11). a_t amplitudes biased with large peaks occurred more in the negative side than in the positive side. The maximum PGA, which occurred at 36.76 seconds, is also associated with the largest deceleration spike of 0.6g at 36.6 seconds. This phenomenon appears to be the result of the maximum PGV as displayed in Chi-2, although the maximum PGA of Chi-26, which occurred at 36.8 seconds, is not kinematically related to the maximum PGV.

Chi-41: Despite the very short strong motion duration in the acceleration records, these three ground motion velocity time histories are quite different. As indicated before, record Chi-41 can be basically identified as the wave propagation from Chi-12 and Chi-22. It has the largest peak velocity of all the 49 records. With maximum PGA ranked 9th among the 49 records, the high velocity was due to a long period

of acceleration interval. Figure 12 shows that shortly before the velocity norm reached 3.2 m/sec, there is a 1.5 seconds long period of continued acceleration. Although the peak amplitude of a_t during this period is only 0.5g, the accumulative effect produced the high level of velocity and displacement (5.4 m). This long period of acceleration can also be identified in Chi-12 and Chi-22, where the corresponding time intervals are 0.35 seconds and 0.75 seconds. Thus this long period of acceleration may not be considered as a local area effect.

Group Three

The records (Chi-42~Chi-49) in this group have much softer soil conditions than that of group one and group two with the shear velocity less than 180 m/sec. The PGA of these records in this group is much lower than that of in group one and group two. This phenomenon gives us an explanation that the ground shaking caused relatively lower response on soft soil site. As examples, Chi-42 and Chi-49 will be examined in more detail.

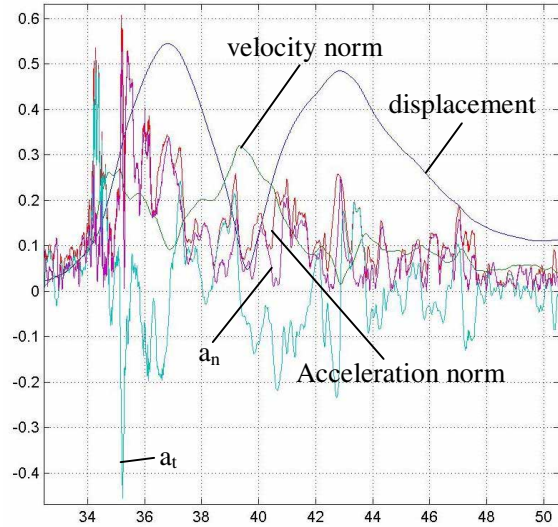


Figure 12 Displacement, velocity norm, tangential a_t and normal a_n of Chi-41

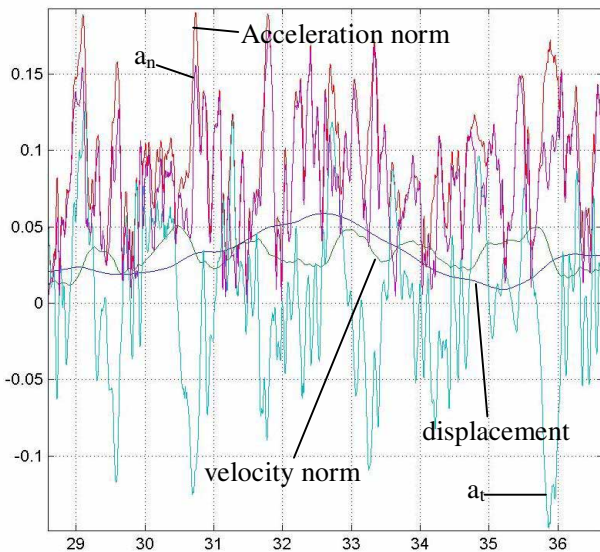


Figure 13 Displacement, velocity norm, tangential a_t and normal a_n of Chi-42

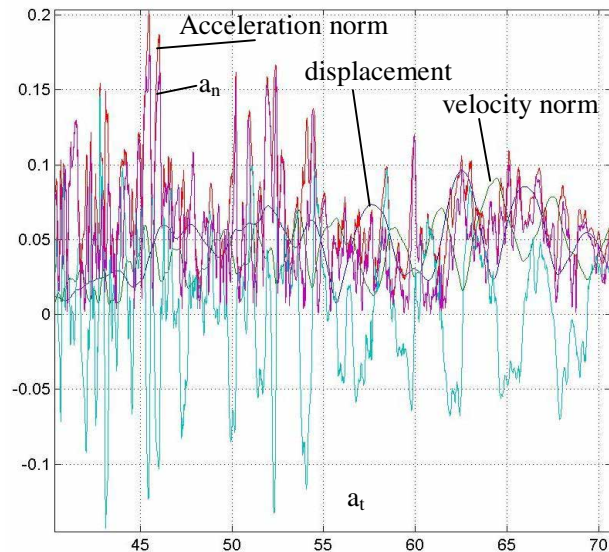


Figure 14 Displacement, velocity norm, tangential a_t and normal a_n of Chi-49

Chi-42: Similar to Chi-41, this record has relatively higher velocity (0.5 m/sec) and displacement (0.66 m) peak value although the PGA is quite low (figure 13). As indicated in the analysis for group one, the decomposed tangential acceleration a_t is also biased to the negative side. Large acceleration spike results in an incremental velocity norm and large deceleration spike results in a rapid decline of the velocity norm. Chi-49 shows much higher velocity norm (0.8 m/sec) and displacement (0.9 m) response (figure 14). This

phenomenon reflects the site effects of soft soil conditions.

CONCLUSIONS

From the above analyses, we may make a number of general observations:

1. The ground acceleration from each station displays some unique dynamic process that had occurred in the local area. These dynamic processes are often reflected by high frequency temporal characteristics. The phenomena expressed through these temporal characteristics vary from one record to another; however, within each record, they often repeat, which indicates the consistency of the dynamic process in the local area. In comparison to the acceleration temporal characteristics, velocity time histories often show more of the ground motion characters that affect a larger area such as wave propagation and attenuation.
2. The relation between maximum PGA and maximum PGV depends on the accumulative effect of acceleration and deceleration. The maximum accumulated effect of the acceleration interval is associated with the maximum PGV. If the maximum PGA is kinematically related to PGV, it must fall into the same time interval which generates the PGV or the time interval immediately follows the maximum PGV.
3. In many of the record studied, the amplitudes of tangential acceleration are biased in the negative side, which indicates that deceleration dominated the PGAs.
4. Study also indicates that there is no obvious difference among the 3D temporal characteristics of ground motions on accelerations but the higher velocity norms and displacement responses roughly reflects the site effects of soft soil conditions.

ACKNOWLEDGEMENT

The authors gratefully acknowledge the joint financial support of the China National Science Foundation through Institute of Engineering Mechanics (50278092) and the US National Science Foundation through Multidisciplinary Center for Earthquake Engineering Research.

REFERENCES

1. Tong, M. and Lee, G. C. (1999), 3D Temporal Characteristics of Earthquake Ground Motion at a Single Point, *Journal of Engineering Mechanics*, ASCE, 1999; 125(10): 1099-1105.
2. Tong, Qi, and Lee (2000), Temporal a_N and a_T in Earthquake Ground Motion Analysis, *Journal of Engineering Mechanics*, ASCE, 2002; 128(5): 502-510.
3. G. C. Lee, M. Tong and R. Tao, Temporal Characteristics of Chi-Chi Earthquake Ground Motion and Their Possible Implications on Structural Damages, *International Workshop on Annual Commemoration of Chi-Chi Earthquake*, Taipei, 2000.